M. Leonard Bryan
W. D. Stromberg
Thomas G. Farr
Jet Propulsion Laboratory
Pasadena, CA 91103

Computer Processing of SAR L-Band Imagery

Digital filtering and thresholding were applied to SAR scenes of sea ice and fresh-water lakes.

Abstract: *A continuing problem with the interpretation of synthetic aperture radar (SAR) data, especially in the image format, is the fact that such radar systems generally are not calibrated. This tends to reduce the validity of computer processing in the form of automatic interpretation as it may be applied to SAR imagery. However, for some classes of targets, i.e., those which have especially constant and high or low returns, such automatic discrimination can be attained easily and quickly by digitally filtering and thresholding the data. We have applied such procedures to two scenes, one of sea ice and the other of fresh-water lakes. The orientation of leads (through a Fourier transform) together with the percentage of open water in the entire sea ice scene is quickly attained. For the lake scene the areas of lakes were determined with a high accuracy by using the standard library routines in a General Electric Image 100 system. These techniques demonstrate the validity of machine processing for obtaining quantitative data for some classes of targets as seen by uncalibrated synthetic aperture radars.*

Introduction

The interpretation of side-looking airborne radar (SLAR) images obtained from either real aperture radar (RAR) or from synthetic aperture radar (SAR) systems has been progressing for the past decade (Dunbar, 1975; Page and Ramseier, 1975). To date, data from a variety of systems operating at numerous frequencies (e.g., K (18-26.5 GHz); K_u (12.5-18 GHz); × (8-12.5 GHz); L(1-2 GHz)) have been interpreted visually. Although there is not a direct transfer of interpretations from one system to that of the next, there is apparently a direct transfer of interpretation methodologies. Hence, it is generally agreed that surface roughness and electrical properties and look and depression angle of the radar are the primary factors controlling the backscatter of incident radar energy and therefore the image brightness. The wavelength of the operating radar is of equal importance in defining these returns.

Present imaging radars lack both a calibration within the entire system and a quantifiable measure of their stability. The former refers to the inability to determine absolute values (such as σ°) of targets and the latter to the repeatability of the values which, although not absolute, may be obtained on subsequent flights over a given target area. Primarily for these reasons, radar interpretation has been largely confined to the mode of photo interpretation dealing with shape, location, time, texture, and relationships to surrounding features. In such a situation, computer processing of radar data is primarily concerned with the enhancement of the target features (e.g., edge enhancement, contrast stretching of intensity).

This does not mean, however, that compu-

Photogrammetric Egineering and Remote Sensing,
Vol. 43, No. 10, October 1977, pp. 1283-1294.

TABLE 1. JPL RADAR SYSTEM PARAMETERS

	L-Band
Transmitted Peak Power	4 kw
Frequency (wavelength)	1215 MHz (25 cm)
Pulse Rep. Frequency	1 KHz at platform V=250 m/sec. velocity
Pulse Width	1.25/μsec.
Bandwidth	10 MHz
Antenna	Phased array 75 × 25 × 5 cm
Polarization	HH, HV; or VV, VH. Range beamwidth 90° centered 45° off vertical. Azimuth 18° centered on zero doppler.
Recorder	Goodyear 102, dual channel, 5″ film.
Areas Resolution	Nominally 25 m × 25 m.

ter processing techniques, in and of themselves, cannot be a major contributor to radar image interpretation (Larson *et al.*, 1974). In some cases the information obtained from computer processing may directly yield results which are either unattainable with other methods or available only through laborious and time-consuming work. This paper describes some of our work in the areas of hydrology and polar ice which define possible uses of automatic picture processing of uncalibrated radar imagery.

THE RADAR SYSTEM AND STUDY AREAS

The data used in this study were collected by the Jet Propulsion Laboratory's (JPL) L-band synthetic aperture radar mounted in the NASA CV-990 aircraft. This radar, the specifications for which are presented in Table 1, was operated at approximately 30,000 feet altitude. Two study areas, one located at 73°30′ N, 140° 00′ W in the Beaufort Sea and consisting of sea ice and the other at 70°30′ N, 156° 00′ W near Admiralty Bay and composed primarily of lakes on the Alaskan North Slope, were used (Figure 1). All were L(HH) data collected on 10OCT75 and 26OCT75 (for the sea-ice scene) and 20OCT75 for the fresh water lake scene.

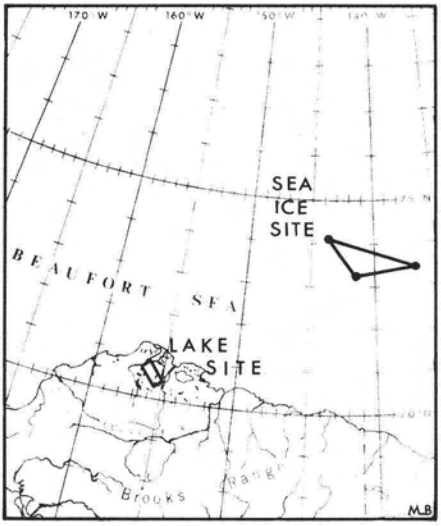

FIG. 1. Location of the study sites used in this work.

APPROACH

From the earlier discussion it follows that picture processing with uncalibrated SAR data is of limited utility although, for certain types or classes of targets, such efforts can yield good results. The targets selected for study should have constant returns almost irrespective of the wavelength or the depression angle of the radar. Because smooth surfaces (e.g., unrippled water surfaces, playa lakes, and mud flats) are always imaged as black "no return" areas (specular reflectors), their automatic discrimination should be quite easy. Other areas of the imagery are also black (e.g., radar shadows) and to discriminate these two classes (smooth from shadows) would be impossible if one were to work only in the automatic picture processing mode. Alternatively, in areas where there is very little topographic relief, and in which the interpreter has some basic conception of the nature of the surface and its configuration, the discrimination of such black areas is relatively simple. Hence, the two areas which have been selected for study consist of some lakes of the Alaskan

North Slope and open water of the Arctic sea ice; both scenes are of areas having very little topographic relief.

In both study areas, following data digitization and thresholding, the percentage of the area which is at any given quantitized grey level can be determined. Also, for the sea-ice study area, through a Fourier transform, it is possible to prepare a rose diagram giving the orientation of the leads.

Difficulties in such a study are few, but are of major importance and must be considered by the interpreter. In the sea-ice case, as ice moves and opens, the water surface is directly visible to the radar imagery and is easily identified. However, if the ice remains stagnant, this water will begin to freeze and thus a thin ice cover, often indistinguishable from the open water on the SAR imagery, will form. It then requires additional amounts of movement to form small ridges (which appear as bright linears) within the thin ice cover to properly identify this new surface. In these cases it is the smoothness of the sea surface (or the smooth surface of the new sea ice) rather than the nature of the surface which is controlling the radar image tone (Bryan, 1976). For such scenes, sequential data are of great importance (Johnson and Farmer, 1971; Ketchum and Tooma, 1973). Seasonality of the data also plays an important role for during the summer months of July to September, when there is surficial melting of the sea ice, smooth melt ponds and increased dampness of the upper surface often combine to give very dark returns. Such returns can be distinguished by using a simple level slicing technique as in this study, but proper identification could not be so easily facilitated.

In the case of the fresh-water lakes and rivers, for data collected at any season other than late winter or spring (February-June), the surface of the water or of the ice will generally be physically smooth. Therefore, imagery of the lake will be black on the SAR data. The oriented lakes, which have resulted from the wind-induced erosion of permafrost on the North Slope, will, during the winter season, have approximately 2 meters of ice on their surfaces. In these areas where the lake has been frozen to the bottom the radar returns will be low; returns will be high for those areas of the lake which are underlain by a water layer. (Elachi *et al.*, 1976; Sellman *et al.*, 1974; Campbell *et al.*, 1975). In the spring, when low density snow ice has developed, and later in the summer when the ice on the small lakes is candeling and disintegrating, the resulting roughness of the lake surface should cause brighter returns on the SAR data. Hence, seasonality of the data collection continues to be of primary importance and the technique we use is best exploited when the lakes are completely ice free, or have new, smooth, and thin covers of crystalline ice. In October, when our data were collected, the lakes were not frozen to the bottom and only very thin and quite homogenous ice covers consisting primarily of black ice overlain by a thin layer of snow existed. Snow ice, which often causes considerable scattering of the radar energy, was not sufficiently developed to affect the backscattering.[1]

A final problem, resulting from the use of uncalibrated SAR data, is that the minimum signal return may be below the radar system noise. Thus, due to variations in the darkroom procedures, it may be possible that system noise appears on the photographic imagery. Such areas, which are physically smooth and theoretically dark on SAR imagery, may have a very low grey tone on the photographic product (Larson *et al.*, 1974).

Study of Arctic Sea Ice

One of the major problems of studying Arctic sea ice is the lack of high-resolution data which have been collected during periods of inclement weather and/or darkness. Efforts at modeling sea-ice movements and at understanding the heat balance problem over the Arctic Ocean are thus hampered by the lack of very basic data concerning the gross movements of the ice and the percentage of open water of the Arctic Ocean. For example, it is noted that seasonal variations in the areal extent of the ice coverage of the Arctic Ocean is about 15 percent (for the Antarctic it approaches 80 percent). These ice-covered sea surfaces thus represent one of the most rapidly moving and varying solid surfaces of the earth, and for studies of ice and ocean dynamics it is of primary importance to know the nature of these movements in both the spatial and temporal domains.

Thus, as stated by Fletcher (1971, pp. 10-11), there is a need:

> . . . to achieve quantitative understanding of the interaction between the fields of motion of the atmosphere, the pack ice, and the liquid

[1] Such scattering is of major importance in passive microwave remote sensing, especially for the detection of aufeis on northern rivers as the Sagavanirktok, Ivishak, and Echooka (Hall, 1976). Discussion of interpretation of SAR data for fresh water lakes is given in Bryan and Larson (1975).

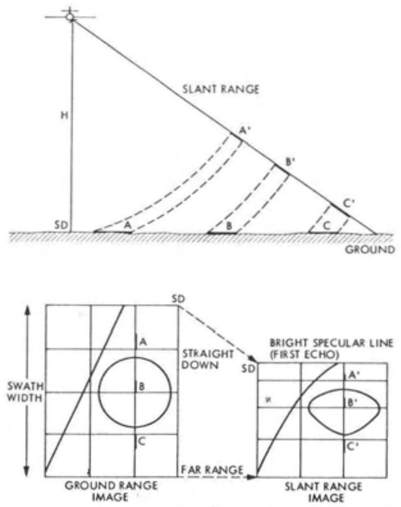

FIG. 2. Geometry of the data obtained by the JPL L-Band Radar.

ocean and to develop the capability to simulate this interaction by means of a mathematical model. The ultimate goal is to predict ice movement and deformation and heat exchange between the ocean and the atmosphere.

The National Aeronautics and Space Administration, in cooperation with several other national agencies and specific projects, has been involved in an Arctic Experiment Program in an effort to obtain such remotely sensed information by using, among other sensors, the JPL SAR. Data presented in this paper were collected during one such project, the Arctic Ice Dynamics Joint Experiment sponsored by the National Science Foundation (Untersteiner, 1974; Weeks *et al.*, 1974; Campbell *et al.*, in press). In order to obtain sufficient areal coverage it was necessary to make multiple passes with the SAR. The SAR views only the right of the aircraft, at an angle extending from nadir to approximately 55°. Thus, from a flight altitude of 30,000 ft. (9144 m) a slant range swath width of approximately 50,800 ft. (15.5 km) would be imaged with each pass. The resulting data were in the slant range mode from which a ground range (map correct) data set could be generated (Thompson *et al.*, 1972) (Figure 2). For this portion of the study we did not conduct that correction; rather, we visually mosaicked all adjacent passes to make the complete (but uncorrected) mosaics of the sea-ice study site which are presented as Figures 3a,3b[2]. As can be seen in these figures, there are some imperfections in the mosaics in that the adjacent strips do not always have sufficient overlap to avoid gaps, and especially in the southern four strips of the 26OCT75 mosaic (Figure 3b) the image outputs of the several data runs were quite different from those of the remainder of the study area. These complete and uncorrected mosaics (Figures 3a, 3b) were optically scanned, digitized on a microdensitometer with a 50 μm sample spacing, and subjected to digital processing to facilitate further analyses.

DIGITAL PROCESSING

Digital processing was performed in the Image Processing Laboratory at JPL with an image processing language and applications software known as VICAR, implemented on an IBM 360/65 computer. The objectives of this work were to:

- improve the subjective appearance (reduce the differences between strips and eliminate the brightness gradient within the strips),
- compute the percentage area comprised of leads and other open water, and
- provide a quantitative measure of the orientation of the leads.

In order to reduce the brightness gradient across each component strip and to equalize their average brightnesses, the mosaics were "high pass" filtered. In general, this operation removes all low spatial frequency variations (i.e., the slowly varying brightness gradient) and sets the average data value to a specified level. However, in the case of these mosaics, the high contrast present between the floes and the leads and also at the edges of the mosaics would have produced an undesirable effect in the filtered images. The effect, sometimes referred to as "ringing," consists of the introduction of opposite polarity shadows on either side of a bright or dark feature. While "ringing" always occurs in "high pass" filtering, its appearance is usually negligible. Only in the presence of high amplitude and abrupt variations, as at the edges of leads or across ridges, does it become objectionable. To avoid "ringing" it was necessary to employ a recently developed, computationally lengthy version of the "high pass" filter which modifies itself in the presence of sharp discontinuities (Schwartz and Soha, 1976). Generally quite

[2] Because the sea ice drifts at approximately 0.3 to 0.5 km per day, it is noted that the geographic coordinates of the sea-ice test site have changed between 10OCT75 and 26OCT75. Close examination of the mosaics reveals that the same area of ice is covered on the two data flights.

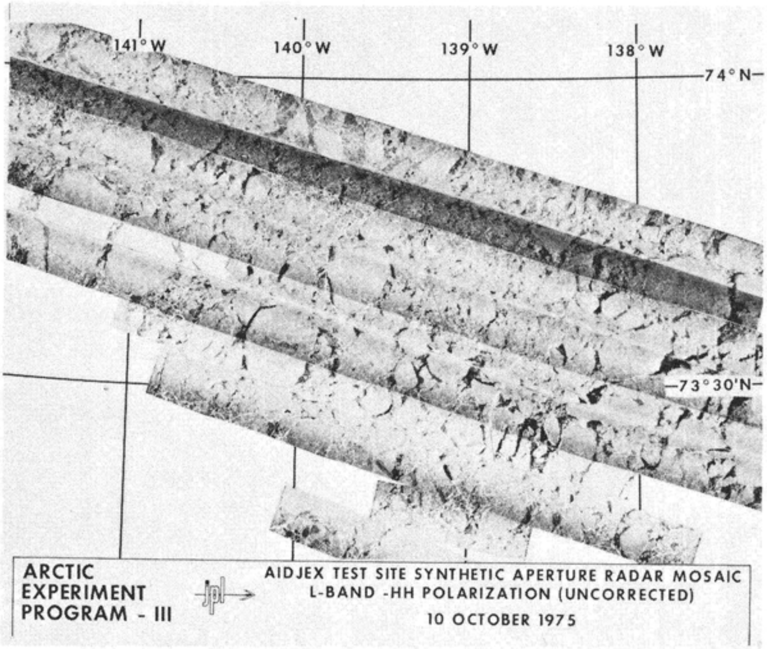

(a)

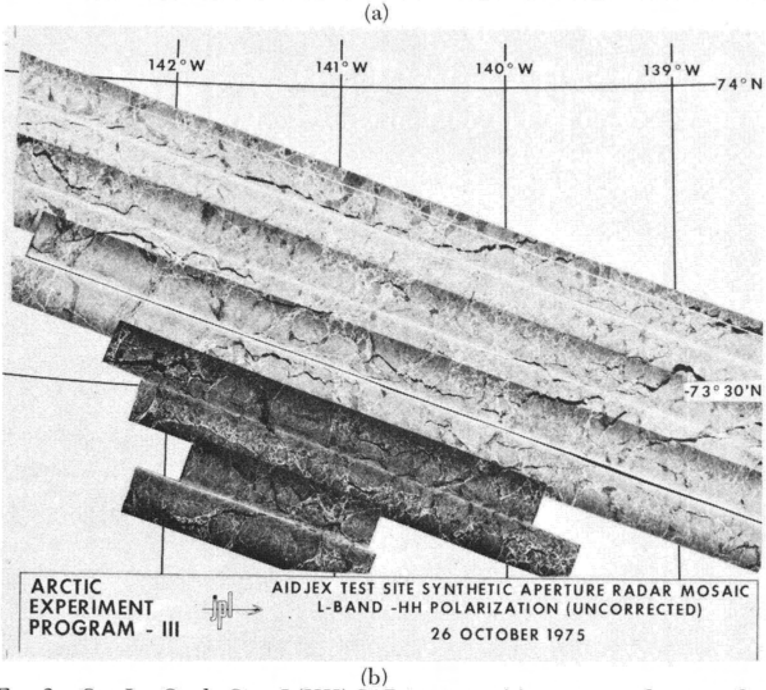

(b)

FIG. 3. Sea Ice Study Site, L(HH) SAR imagery: (a) uncorrected mosaic for 10OCT75, (b) uncorrected mosaic for 26OCT75.

successful results, Figure 4(a,b), were obtained with this adaptive filter. However, some residual "ringing" is apparent at the right of both mosaics near the locations of the geographic coordinates seen in Figure 3. Further adjustment of the control parameters in an additional application of the filter could have reduced the severity of the effect, but the cost was not felt to be warranted in view of the limited extent of the phenomenon.

Application of the "high pass" filter made possible the isolation of the leads by simple brightness thresholding. In order to deter-

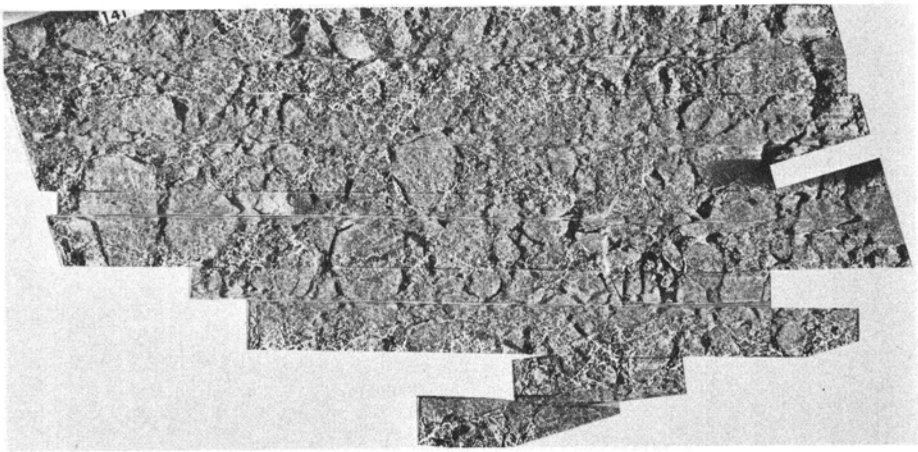

(a)

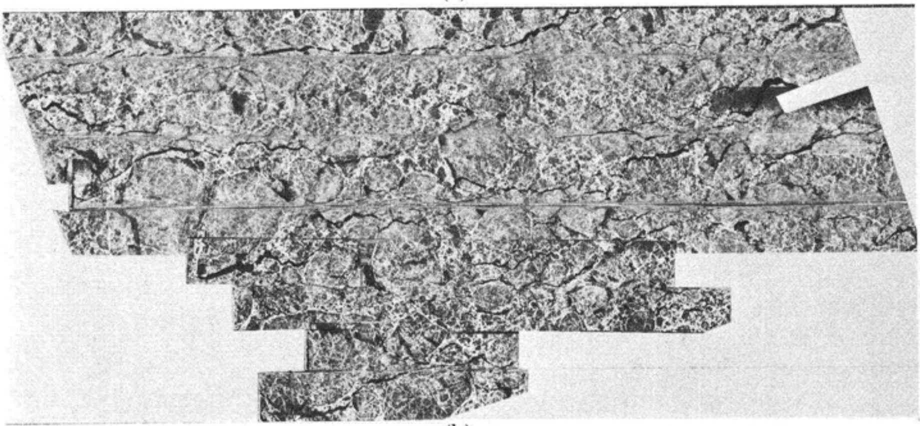

(b)

FIG. 4. The results of high pass filtering Figure 3: (a) filtering of Figure 3a, 10OCT75, (b) filtering of Figure 3b, 26OCT75.

mine a level which would separate open water and thin ice from other ice types, images thresholded at several candidate brightness values were generated and compared with the filtered mosaics. An intensity transformation which mapped all brightness values less than the threshold to one value and those above to another value was then undertaken. The binary images thus generated are displayed in Figure 5. The percentage of area occupied by leads was obtained from histograms of the binary images with adjustments to compensate for the irregular marginal areas surrounding the mosaics. The area imaged and represented in Figure 5a and 5b are 8,472 km^2 and 8,020 km^2 respectively. Leads comprised 1.6 percent of the area for 10OCT75 (Figure 5a) or 136 Km^2 and 1.1 percent or 88 Km^2 for the study area for 26OCT75 (Figure 5b).

A measure of the orientation of the leads was obtained through automated examination of the Fourier transforms of the binary lead pictures. The relative contribution of Fourier components within one degree intervals was determined by integrating the amplitude of the Fourier transform over consecutive one degree pie-shaped wedges. A linear feature produces a long narrow mound, oriented in the same direction as the feature, in the amplitude of its Fourier transform. The cumulative effect of a non-uniformly distributed, randomly oriented set of features is to generate a transform amplitude surface which has larger amplitude along some radii than others. Therefore, by radially integrating in the transforms of the binary lead images, the proportion of components at each orientation was obtained. Polar plots of these integrals are displayed in Figures 6(a,b). The radial distance to the curve represents the proportion of leads parallel to the radius.

APPLICATIONS OF PROCESSING OF SEA ICE SCENES

Because a satellite borne imaging radar system will have predetermined orbits, and

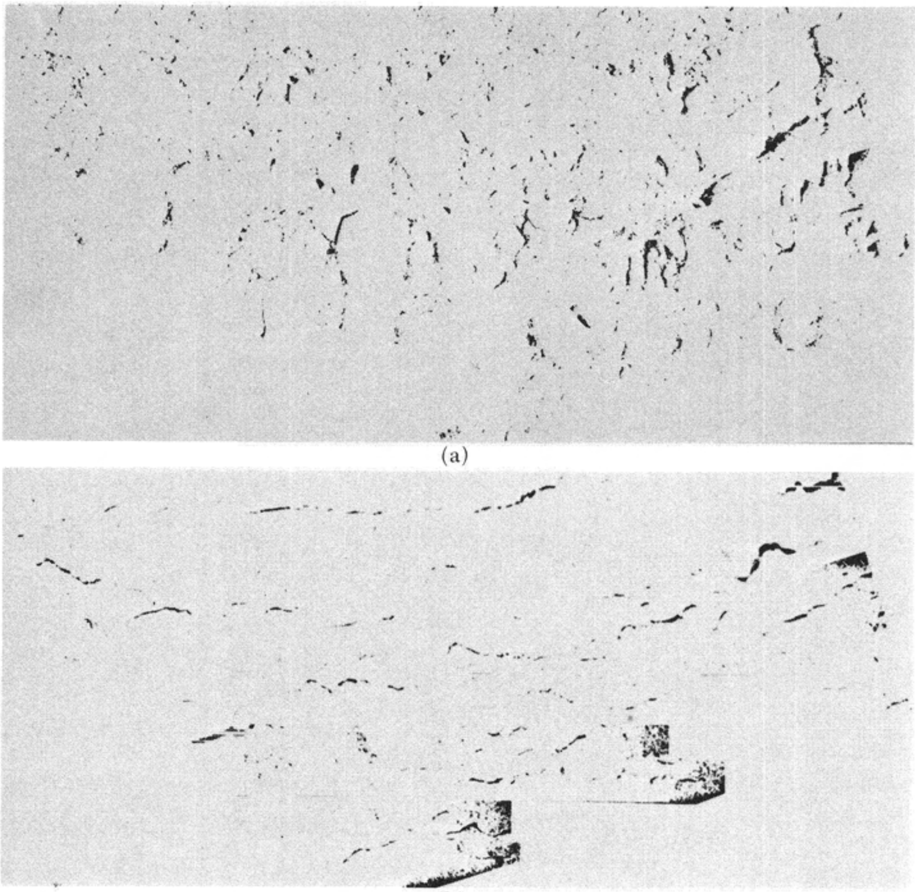

FIG. 5. The results of thresholding the high pass filtered images shown in Figure 4: (a) for 10OCT75, dark areas representing leads and other open water areas, constitute 1.6 percent of the entire scene, (b) for 26OCT75, dark areas representing leads and other open water areas,

given that such a system will be polar orbiting, radar imagery of sea ice similar to that used in this study will become available. These data will be available for each satellite pass, assuming the sufficient collection and storage abilities of the orbiting radar. Seasat radar, for example, will probably provide better data than we have used because its swath width will be approximately 199 km. This will yield a coverage similar to that provided by our entire mosaic and reduce the processing problems by removing the need for the first (brightness equalization) picture processing operation.

Through the remaining digital processing techniques we can obtain information concerning the gross movements of sea ice through time. Changes in both the percentage of dark areas (which represent open water and recently refrozen leads) and the orientation of these areas will allow the oceanographer to quickly identify areas of major ocean and ice dynamics. By creating a set of sequential data for several geographic areas of the polar seas a hierarchy of zones of progressively intense oceanic activity in both the space and time dimensions can be developed. An increased understanding of ocean dynamics will be available to scientists developing mathematical models dealing with heat balance, physical oceanography, and oceanic circulation of the polar seas by using such data sets.

As an example of the nature of the synoptic energy budgets over the Beaufort Sea, we summarize Vowinckel and Orvig (1971):

- The "oasis effect," that is, irregularities in conditions over even the most uniform surface types are quite pronounced in the Polar Oceans;
- For polar oceans, absorbtion of short-wave radiation is higher over open water than over ice; but the total energy losses are greater over open water than over ice, and

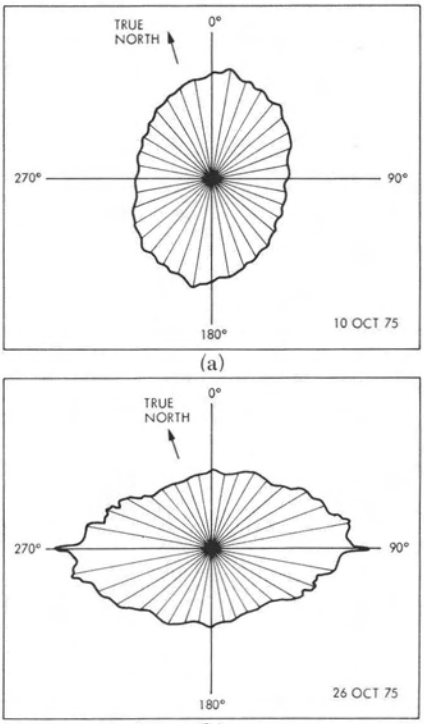

FIG. 6. Polar plots of the Fourier transform performed on Figure 5. Radial distances to the curve from the origin represent the proportion of leads and other open water areas within the scene which are parallel to that radius: (a) for 10OCT75, (b) for 26OCT75.

this additional loss is supplied by the ocean water itself (e.g., the sensible heat flux over water is 63 times that over ice at the same time, and of an opposite sign (for February));

- Open water areas are not negligible with respect to the assessment of regional values for the turbulent flux, and under certain conditions the direction of the areal net flux may be determined by a few percent of open water (Table 2);
- Compared to the importance of open water, the ice thickness is of minor consequence; and
- Thus, it is concluded that, "... the ice covered Polar Ocean is a heat sink during the whole year as are also the open water areas during summer. During winter, however, the open water spots present great heat sources."

The implications with respect to synoptic air mass meteorology are obvious.

At present, vast areas of the open ocean, and for extensive periods of time, are essentially unknown with respect to their true ocean dynamics. The inclusion of satellite borne active microwave data, such as we have used in this study, will help fill these information gaps.

One additional comment must be made. We note that the discrimination of the areas yielding very low backscatter is relatively simple, but the correct identification of such areas is somewhat more difficult. Although data concerning microwave emissivity from ice and open water are quite unambiguous (open water having emissivities approximately 50 percent of that of ice at 3.0 and 1.0 cm wavelengths (Wilheit *et al.*, 1972)), such data collected from satellite altitude by microwave radiometers have low resolutions (in the neighborhood of 32 km).[3] Thus it appears that the best system for correct identification of ice types and percentage of open water is to combine the all-weather capabilities of the two (active and passive) microwave systems in which the SAR provides the very high resolution while radiometers provide accurate surface type identification (Campbell *et al.*, 1975). This will allow the development of algorithms for interpretation of pixels having intermediate brightness temperatures in the radiometer data (such as presently received by the Nimbus satellite series), with the SAR being used to give data concerning percentage of ice coverage of the given Nimbus data pixel.

STUDY OF NORTH SLOPE LAKES

The radar cross-section of land is generally higher and more varied than that of the ocean's surface (Long, 1975). This creates some basic problems with respect to computer processing of uncalibrated radar data of land scenes. The wide variety of returns, and the close juxtaposition of the strength of the backscatter in both space and intensity, requires that we again seek features which have fairly constant returns. As discussed previously, fresh-water surfaces, liquid or frozen (assuming that the latter are not frozen to the bottom), are very good candidate surfaces for this study.

Such features, even on the Alaskan North Slope, are of both practical and scientific interest. With the development of this area, especially with respect to oil exploration, there is a need for water supplied for both industrial and domestic use. Also, because surface travel during the summer is quite rigorous, it has been suggested that it would be economical to use frozen lakes as airfields

[3] Mircowave radiometers on Nimbus G and the Seasat SMMR, operating at 37 GHz, will have a resolution of 25 km by 16 km for the elliptical footprint.

TABLE 2. THE PERCENTAGE OF THE OCEAN SURFACE, IF OPEN WATER, WHICH WILL GIVE AN ENERGY LOSS EQUAL TO THAT FROM THE REMAINING ICE COVERED SURFACE (VOWINCKEL AND ORWIG, 1971, p. 156).

OCTOBER	NOVEMBER	DECEMBER	JANUARY	FEBRUARY	MARCH	
5.2	2.4	0.8	0.1	0.1	0.2	%

to support winter drilling and exploration parties (O'Lone, 1975). Hence, we feel that there are needs for continuing the study of the information extractable from remotely sensed data, including SAR data, of these areas.

DIGITAL PROCESSING

For this portion of the study the original SAR data were scanned at 40 μm aperture, geometrically corrected (Figure 7), and processed by using a General Electric Image 100 multispectral analyzer. The returns from the lakes were low (being horizontal specular reflectors). These were enhanced, with respect to the surrounding terrain, by the linear contrast stretch program. The lakes were then separated from the surrounding terrain by a density slicing technique and stored in the theme storage areas. Nineteen lakes within the candidate scene, varying in size from 0.54 km^2 to 6.09 km^2, were selected and isolated for study[4]. Each lake was individually measured using a pixel count and a map of the several lakes printed. Figure 8 shows the print-out of the selected lakes as identified on the Image 100. The question to be answered deals with the accuracy with which this method, using a simple thresholding technique applied to uncalibrated L-band SAR data, can be used to measure the area of each of the several lakes. It was determined, given the resolution of the radar, the aperture size used for scanning, and the processing system, that each pixel on the Image 100 represented an area of 900 m^2. Hence, we were able to determine directly the areal extent of each lake. As a check, the 1:250,000 map of the study area (Teshekpuk, Alaska) was used to obtain surface areas of the lakes. Figure 9 gives these relationships.

APPLICATION OF PROCESSING OF LAKE SCENES

The technique of using the Image 100 and the thresholding programs to analyze uncalibrated SAR L-band data has provided us with an accurate and quick measurement of the surface areas of the lakes of the northern Alaskan tundra. The differences between the areas detected by the computer technique and that using the manual (planimeter) technique can be partially attributed to the scale of the map used and the fact that the 1:250,000 map was 15 years older than the SAR data. Ideally, aerial photography would have been the best source of comparative data, but these were not available for this study. Also, Landsat (especially Bands 6 and 7) would provide accurate comparative data.

If we consider these lakes as flooded areas, it is suggested that uncalibrated L-band SAR data similar to that used in this study and which will be available from satellites (such as Seasat) can be used to identify such areas in many land scenes. Because of the all-weather capabilities of radar, studies of floods can be conducted, in an automatic processing mode, while the floods are in progress. Some difficulties can arise (e.g., differentiating shadows and similar dark or no-return areas from floods in rough terrain, and possibly separating flat terrain from adjacent flooded areas) and it is in such situations that both sequential data and the previous knowledge of the interpreter of the general scene will be of major importance in facilitating accurate interpretation. Earlier work in the comparison of infrared photography, bands 6 and 7 of Landsat data, and synthetic aperture radar has shown the relationships of these data sets with respect to flooded terrain. By combining these additional sets, accuracy of interpretation, either automatic or manual, can be improved (Bryan, 1975b).

CONCLUSIONS

Because the strength of radar backscatter for a variety of scenes is quite varied, it is desirable that calibrated SAR data be made available for earth resources purposes. Nonetheless, certain types of features, those which have very constant returns which are

[4] Lakes of smaller sizes were easily measured from the SAR data using the Image 100, but the accuracies of the planimeter measurements for such small areas, and at the scale of 1:250,000, were in doubt. Therefore, these were not included in this study.

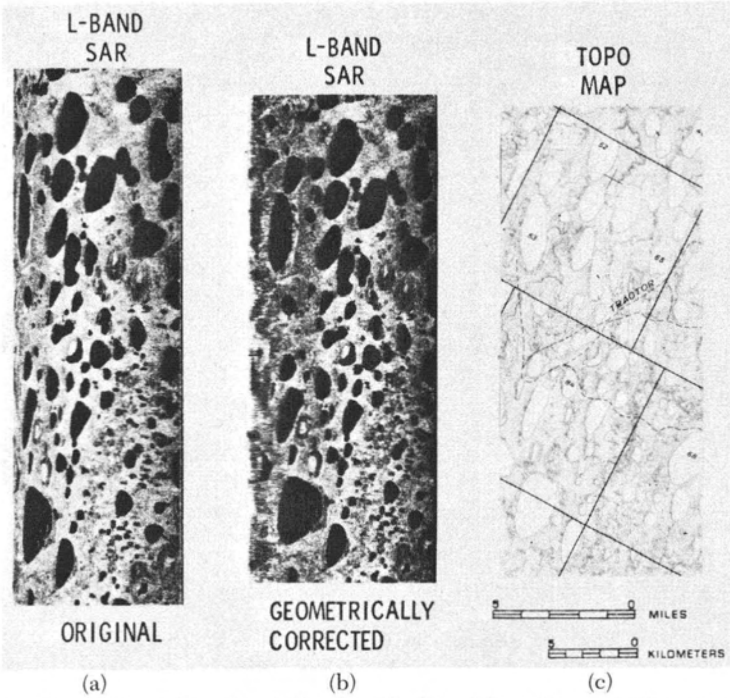

FIG. 7. Data used in the study of north slope lakes: (a) raw SAR L(HH) imagery, (b) geometrically corrected SAR L(HH) data, and (c) portion of 1:250,000 topographic map used for comparison.

also very high or very low in intensity,[5] can be efficiently studied by using simple automatic picture processing techniques applied to uncalibrated radar data. Thus, in areas which are generally inaccessible or in which monitoring of the changes of some types of earth's surfaces (such as polar sea ice, arctic tundra, or areas of flooding) are required, such uncalibrated SAR data can provide earth scientists with valuable information for modeling and mapping functions. Obviously, combinations of multifrequency, multipolarization, sequential, and calibrated SAR data will allow the extension of these techniques. Similarly, the inclusion of additional wavelengths beyond the microwave or additional modes of microwave remote sensing (i.e., passive) together with additional and more sophisticated digital processing techniques may be employed and will obtain accurate results.

[5] Examples of high backscatter scenes for which this technique may be employed are the commercial and industrial (including strip commercial) areas within urban scenes. The high point returns and their close proximity to one another in space and time renders these areas easily identifiable (Bryan, 1974, 1975a).

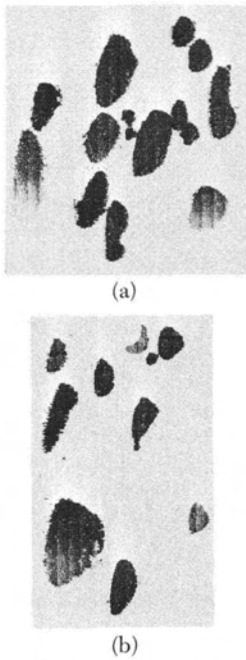

FIG. 8. Identification, using Image 100, of the several lakes selected for study. (a) Northern portion of study site seen in Figure 7c, (b) Southern portion of study site seen in Figure 7c.

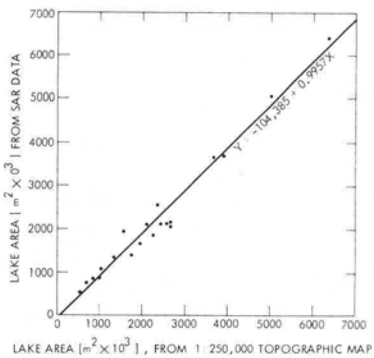

FIG. 9. Comparison of areas of lakes within study site as determined by planimetric measurements on 1:250,000 maps and using the Image 100. Least squares relationship is shown.

ACKNOWLEDGMENTS

The authors wish to thank R. O. Ramseier, Canadian Department of Environment; D. K. Hall of Goddard Space Flight Center; and D. Harrison, S. Scott, E. McMillian, D. Baker, and K. Borger (all of JPL) for their contributions and helpful comments during the conduct of this work. They also would like to thank the Ames Airborne Science Program Office for the support in the data collection. The work has been funded by the EODAP office as part of the AIDJEX support.

This paper presents the results of one phase of research carried out at JPL, California Institute of Technology, under contract NAS7-100, sponsored by the National Aeronautics and Space Administration.

REFERENCES

Bryan, M. L., 1974. Extraction of Urban Land Cover Data from Multiplexed Synthetic Aperture Radar. *Proceedings,* 9th Intl. Symp. Remote Sensing of Environment, Ann Arbor, MI., Env. Res. Inst. MI., pp. 271-288.

————, 1975a. Interpretation of an Urban Scene Using Multichannel Radar Imagery. *Remote Sensing of Environment,* V. 4, No. 1, pp. 49-66.

————, 1975b. Flooding of Monroe County, Michigan: A Comparison of Three Remote Sensor Data Sets. *Michigan Academician,* V. 8, No. 4, pp. 425-440 (also: NTIS N75-21738).

————, 1976. Interpretation Key for SAR (L-Band) Imagery of Sea Ice. *Proceedings,* Am. Soc. Photogrammetry, Fall Convention, pp. 406-435.

Bryan, M. L., and R. W. Larson, 1975. The Study of Fresh-Water Lake Ice Using Multiplexed Imaging Radar. *J. Glaciology,* V. 14, pp. 445-457.

Campbell, W. J., R. O. Ramseier, W. F. Weeks, and P. Gloersen, 1975. An Integrated Approach to the Remote Sensing of Floating Ice. *Third Canadian Symp. on Remote Sensing,* Sep., pp. 39-72.

Campbell, W. J., *et al.* (in press). Microwave Remote Sensing of Sea Ice in the AIDJEX Main Experiment. *J. of Boundary Layer Meteorology.*

Dumbar, M., 1975. *Interpretation of Sea Ice in Nares Strait and the Arctic Ocean. J. Glaciology,* No. 73, pp. 193-213.

Elachi, C., M. L. Bryan, and W. F. Weeks, 1976. Imaging Radar Observations of Frozen Arctic Lakes. *Remote Sensing of Environment,* V. 5, #3, pp. 169-175.

Fletcher, J. O., 1971. Probing the Secrets of Arctic Ice. *Naval Research Reviews,* V. 24, No. 3, pp. 9-24.

Hall, D. K., 1976. Analysis of Some Hydrologic Variables on the North Slope of Alaska Using Passive Microwave, Visible and Near Infrared Imagery. *Proceedings,* Am. Soc. Photogrammetry, Fall Convention. pp. 344-361.

Johnson, J. D., and L. D. Farmer, 1971. Use of Side-Looking Airborne Radar for Sea Ice Information. *J. Geophysical Res.,* V. 76, pp. 2138-2155.

Ketchum, R. D. JR. and S. G. Tooma, JR., 1973. Analysis and Interpretation of Air-Borne Multi-frequency Side-Looking Radar Sea Ice Imagery. *J. Geophysical Res.,* V. 78, pp. 520-538.

Larson, R. W., *et al.,* 1974. Multispectral Microwave Imaging Radar for Remote Sensing Applications. *Proceedings,* Specialist Meeting on Microwave Scattering and Emission from the Earth. Berne, Switzerland, Universitat Berne, 23-26 Sep. 1974, pp. 305-315 (Available: AIAA #A75-33881).

Leberl, F., T. Farr, M. L. Bryan, and C. Elachi, 1976. Study of Arctic Sea Ice Drift from L-Band Synthetic Aperture Radar. *Proceedings,* Am. Soc. Photogrammetry. Annual Meeting. pp. 597-611.

Long, M. W., 1975. *Radar Reflectivity of Land and Sea.* Lexington, Ma. Lexington Books. xxvi + 366 pp.

O'Lone, R. G., 1975. Alaskan Air Support Facing Challenges. *Aviation Week and Space Technology,* V. 103, No. 23, pp. 14-17.

Page, D. F., and R. O. Ramseier, 1975. Application of Radar Techniques to Ice and Snow Studies. *J. Glaciology,* V. 15, No. 73, pp. 171-195.

Schwartz, A., and J. Soha, 1976. *Variable Threshold Zonal Filtering.* (JPL Report to be published)

Sellman, P. V., W. F. Weeks, and W. J. Campbell, 1975. *Use of Side-Looking Radar to Determine Lake Depth on the Alaskan North Slope.*

Hanover, N.H., Cold Regions Res. and Eng. Lab. Special Report No. 230, 6 pp.

Thompson, T. W., R. S. Bishop, and W. E. Brown, JR., 1972. Progress Report on 25 cm. Radar Observations of the 1971 AIDJEX Studies. *Aidjex Bulletin*, No. 12, pp. 1-15.

Untersteiner, N., 1974. Arctic Ice Dynamics Joint Experiment. *Arctic Bulletin*, V. 1, No. 4, Spring, pp. 145-159.

Vowinckel, E., and S. Orvig, 1971. Synoptic Energy Budgets from the Beaufort Sea: in WMO Technical Note 129, *Energy Fluxes Over Polar Surfaces*. Also in *Proceedings* of the IAMP/IAPSO/SAR/WMO Symposium. Mowcow, 03-05 Aug. 1971, pp. 143-166. NTIS: N74-17343.

Weeks, W. F., M. D. Coon, and W. J. Campbell, 1974. The Remote Sensing Program Required for the AIDJEX Model. *Aidjex Bulletin*, V. 27, Nov., pp. 22-44.

Wilheit, T., W. Nordberg, J. Blinn, W. Campbell, and A. Edgerton, 1972. Aircraft Measurements of Microwave Emission from Arctic Sea Ice. *Remote Sensing of Environment*, V. 2, No. 3, pp. 129-139.